Phonon spectra and vibrational mode instability of $MgCNi_3$

Prafulla K. Jha
Computational Condensed Matter Physics Laboratory, Department of Physics, Faculty of Science, The M.S. University of Baroda, Vadodara-390 002, India

(Received 21 July 2004; revised manuscript received 19 October 2004; published 6 December 2005)

This paper reports a detailed and systematic lattice dynamical calculation of the newly discovered intermetallic superconductor $MgCNi_3$ by using a lattice dynamical model theory based on pairwise interactions under the framework of the rigid ion model. The results bring out the anomalous vibrational mode instability in the phonon dispersion curves and phonon density of states of $MgCNi_3$. The calculated phonon dispersion curves and phonon density of states are in good agreement with the measured and density functional theoretical (DFT) data. The study also illustrates the contradicting results on the magnitude of phonon frequencies due to Mg atoms and the region of the unstable modes in the Brillouin zone of the previously computed two DFT results. The present study on DOS has enabled an atomic level understanding of the phonon density of states. The phonon density of states has been used to compute the specific heat at constant volume. The Debye temperature and temperature-dependent vibrational amplitudes of the different species are also reported. The present calculation suggests that the superconductivity in $MgCNi_3$ is governed by the BCS mechanism.

DOI: 10.1103/PhysRevB.72.214502 PACS number(s): 63.10.+a, 63.20.−e, 74.25.Kc

I. INTRODUCTION

The recent discovery of superconductivity in intermetallic $MgCNi_3$ at temperature near 8 K (Ref. 1) has generated great interest because of its unusual characteristics in the recently found series of superconductors. This perovskite superconductor is special because oxide and copper are not present. Although, the superconducting transition temperature (T_c) for this compound is too low from an application point of view, the high content of Ni suggests a ferromagnetic ground state and magnetic interactions which may be an important indicator of the existence of superconductivity in this compound. Since the discovery of superconductivity in $MgCNi_3$ there are speculations that the magnetic interactions might play a role in the superconductivity mechanism.[2] However, the temperature-dependent measurement of specific heat[3] and NMR (Ref. 4) suggest that the $MgCNi_3$ is a conventional (BCS) superconductor. On the other hand, tunneling[5] and microwave impedance[6] measurements support the non-*s*-wave pairing mechanism (unconventional or non-BCS superconductivity). Volker and Sigrist[7] have suggested a theoretical picture for a plausible explanation of these contradictory experimental results under the framework of the BCS mechanism which assumes that $MgCNi_3$ is a multiband material. A recent specific-heat capacity study of the Zn-doped $MgCNi_3$ concludes that the $MgCNi_3$ is a BCS superconductor.[8] Also, $MgCNi_3$ with the cubic perovskite structure is similar to the superconducting nickel borocarbides (particularly for the Y and Lu compounds) which show a pronounced softening in the acoustic phonon branch at lower temperatures, a feature supposed to be connected to the superconductivity in this class of compounds.[9–16] From a recent x-ray absorption study[17] and linear muffin-tin-orbital (LMTO) calculation[18] unusual lattice dynamical properties of $MgCNi_3$ compound have been observed, which indicate deviation of the local atomic structure from the ideal perovskite lattice at temperatures below 70 K. To understand the role of lattice distortion or dynamical instabilities in $MgCNi_3$, Ignatov *et al.*[17] have investigated and compared the structure of $MgCNi_3$ with the well researched isostructural $Ba_{0.6}K_{0.4}BiO_3$ (Refs. 19 and 20) for which it is generally an accepted fact that the electron-phonon coupling plays at least a partial role in superconductivity. They have concluded that the electron-phonon (*e-p*) interaction is stronger in $MgCNi_3$ than $Ba_{0.6}K_{0.4}BiO_3$. However, they emphasized for a detailed and systematic study of phonons and their relation with electrons in the $MgCNi_3$ compound. Heid *et al.*[21] in their temperature-dependent inelastic neutron scattering (INS) measurements of the generalized phonon density of states (GDOS) observed a softening of low-frequency Ni modes. To analyze the INS data they performed first-principles density functional theoretical calculations and reported the results on the phonon density of states and phonon dispersion curves for stoichiometric $MgCNi_3$ in selected symmetry directions.[21] Both the DFT calculated phonon dispersion curves[18,21] and the generalized DOS of Heid *et al.*[21] show softening of acoustic phonon modes, but there are contradictions in the magnitude of the frequency of Mg atom vibrations and the area and position of unstable modes in the Brillouin zone. The electronic structure calculation of Shim *et al.*[22] using the LMTO band method with the local density approximation (LDA) and Singh and Mazin[23] using the linearized augmented plane wave (LAPW) method with LDA suggest that the superconductivity in $MgCNi_3$ can be described by the conventional BCS mechanism, however, they emphasized for a systematic and detailed study of phonon properties of $MgCNi_3$. Hence, at this juncture, it seems necessary to perform precise numerical calculations for phonon properties to clarify the role of phonons and understand the superconductivity mechanism in $MgCNi_3$. This paper presents results of a detailed and systematic investigation of phonon properties by using a lattice dynamical model theory, which considers the pairwise atom-atom interactions consisting of Coulombic and short-range repulsive potentials in the

TABLE I. Interatomic potential parameters derived for $MgCNi_3$ at 300 K: r_{cutoff}=20 Å.

Short-range interactions			Effective charge	
Interactions	a (eV)	b (Å)	Ion	Z
Mg-C	1376.06	0.3834	Mg	1.02
C-Ni	1241.40	0.3014	Ni	−3.0
C-C	2425.16	0.2763	C	−1.98

framework of a rigid ion model. It is indeed essential to find out if the present simple model based on interatomic interaction is sufficient to describe the vibrational properties of the $MgCNi_3$ compound. The paper is organized as follows. In Sec. II we describe the interatomic potential in the rigid ion model. In Sec. III we present results and a discussion followed by a conclusion in Sec. IV.

II. INTERATOMIC POTENTIAL AND THEORY

The calculation of phonon properties reported in the present paper for intermetallic superconductor $MgCNi_3$ is performed by using a lattice dynamical model theory, namely, the rigid ion model. This model considers the ionic interactions by sums of long-range Coulomb potentials and short-range potentials, the latter usually chosen based on the pairwise interaction consisting of exponential form. The potential function can be expressed as

$$V(r) = \left(\frac{(Ze)^2}{4\pi\varepsilon r}\right) + ae^{-(b/r)}. \quad (1)$$

In Eq. (1) the first term is the Coulomb potential, the second term is the short-range potential, and r is interatomic separation. The value of constant $(e^2/4\pi\varepsilon)$ is 14.4 eV Å. Z is the effective charge of the atoms and is treated as a parameter. The charge neutrality of the unit cell is maintained. The values of short-range potential parameters a_{ij} and b_{ij} for each pair of atoms are usually found by fitting to the experimental data and ensuring that the stress and forces on all atoms for the given structure vanish. In the present study, in principle, no fitting of the experimental data (phonon frequencies) is done to obtain the parameters due to nonavailability. However, it is ensured that the physically significant parameters are obtained which give nearly vanishing forces on all the atoms and the right magnitude of the eigenfrequencies in the harmonic approximation. For the right magnitude of the eigenfrequencies, guidance has been taken from INS data (Mg atom vibrational frequencies).[21] It is noted that no data have been used at all for the fitting but only used as a guide whether the obtained eigenvalues are correct or not in the harmonic approximation. In the present investigation, only the nearest-neighbor repulsive interactions are considered to contribute to the non-Coulombic part of the dynamical matrix. To calculate the phonon properties, the software LADY for lattice dynamical simulation is used.[24] The parameters so obtained are listed in Table I.

TABLE II. Zone center optical phonon frequencies of $MgCNi_3$. All modes are triply degenerate.

Mode	Type	Frequency (cm^{-1})
F_{1u}	IR	192
F_{1u}	IR	280
F_{1u}	IR	605
F_{2u}	IR	147

III. RESULTS AND DISCUSSION

For the present calculations of phonon properties, $MgCNi_3$ of cubic structure (space group $O_h^1, Pm\bar{3}m$) with a lattice constant of a=3.81 Å[1] and the structural parameters Mg at (0,0,0), C at (0.5,0.5,0.5), and Ni at (0.5,0.5,0), (0.5,0,0.5), and (0,0.5,0.5) is considered. According to symmetry analysis the ideal perovskite of cubic structure presents 12 zone center optical phonon modes. These modes correspond to the following irreducible representations at the zone center:

$$\Gamma(O_h^1) = 3F_{1u} + F_{2u}. \quad (2)$$

The three F_{1u} and one F_{2u} irreducible representations are the infrared (IR) active optical phonon modes allowed for cubic symmetry. As a perfect perovskite of cubic structure all lattice sites have inversion symmetry; first order Raman scattering is forbidden. The zone center optical phonon frequencies calculated by using the above-mentioned lattice dynamical model are presented in Table II. Figure 1 depicts the shapes of these IR active modes. Since, no experimental IR spectra or calculated IR active phonon modes for $MgCNi_3$ are available, comparison could not be made. Noting the success in reproducing the phonon dispersion curves and generalized phonon density of states presented below, however, it can be assumed that these calculated frequencies at zone center will be in good agreement with the experimental data when they are available in the future.

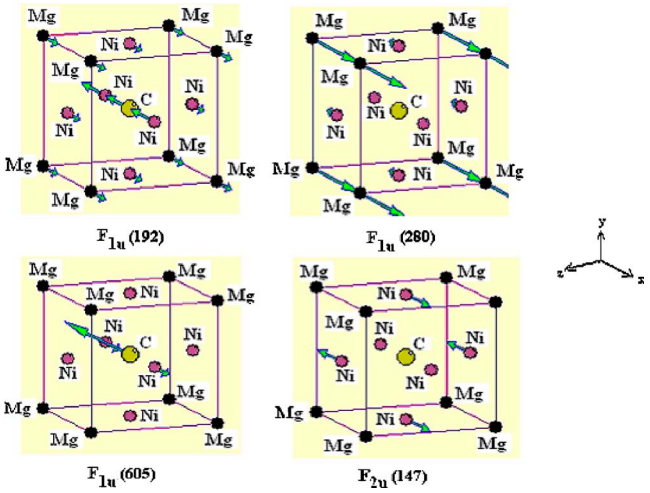

FIG. 1. (Color online) Schematic representation of the shape of the IR active phonon modes.

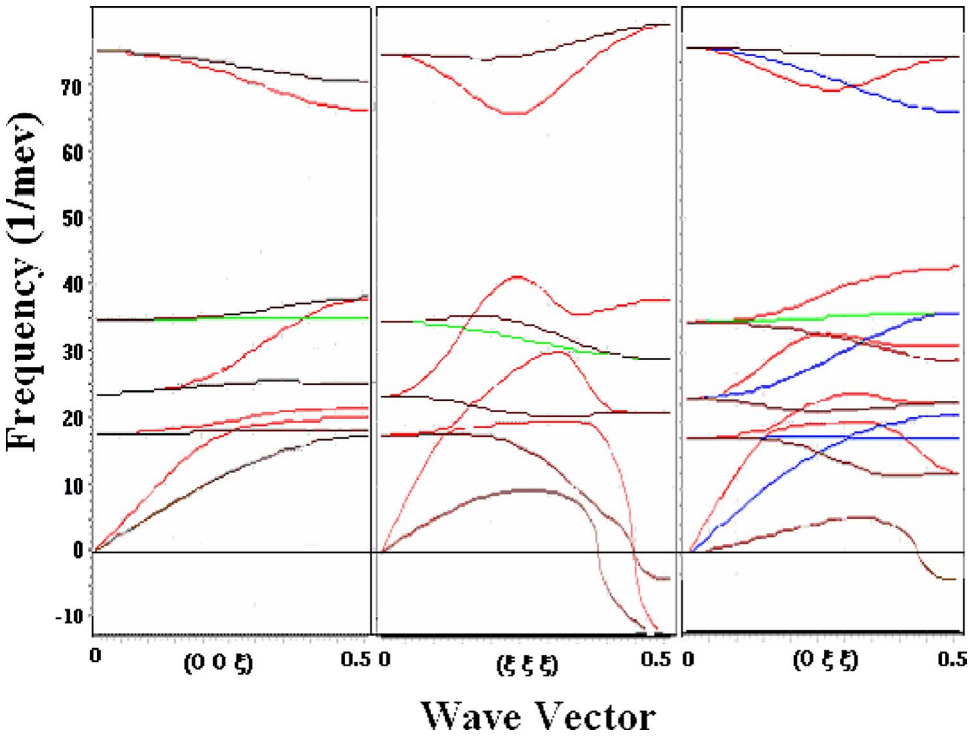

FIG. 2. (Color online) Calculated phonon dispersion curves for $MgCNi_3$ along the three high symmetry directions of the Brillouin zone.

Since the main issue in the $MgCNi_3$ compound is lattice instability, which is reflected in the phonon dispersion curves and phonon density of states, the phonon spectrum along major high symmetry directions of the cubic Brillouin zone are calculated and presented in Fig. 2. As there are 5 atoms in the unit cell, there are 15 phonon modes along each direction. Figure 2 reveals that the phonon branches are distributed almost uniformly up to about 35 meV (280 cm^{-1}) in all three high symmetry directions. A critical assessment of the PDC reveals that there are three regions in which phonon modes are distributed. The top regions at about 77 meV consisting of three phonon branches are due to the carbon atom vibrations, the middle three branches at about 35 meV are due to the Mg atom vibrations, and the lower nine branches are due to Mg and Ni atom vibrations. A similar description of the phonon dispersion has been given by Ignatov *et al.*[18] from their DFT calculation. As far as the most prominent and remarkable feature, the unstable low lying acoustic modes predicted by the DFT calculations,[18,21] is concerned, the present simple model reproduces them quite satisfactorily except few minor deviations. The present calculation is able to produce the unstable modes at zone boundary points in (**qq0**) and (**qqq**) directions of the Brillouin zone (BZ). This instability of modes appears over a large area in the reciprocal space similar to the DFT calculations.[18,21] The mode responsible for the instability of the lattice is due to the vibrations of Ni atom normal to the Ni-C bond and perpendicular movements of two Ni atoms towards octahedral mode of four Ni atoms and two Mg atoms. However, Fig. 2 reveals that the present phonon dispersion curves are slightly different from the DFT calculations[18,21] particularly in predicting the positions of the unstable modes in BZ. While the present model fails in predicting the instability of low-lying phonon modes in the (**q00**) direction of the BZ, it predicts the instability of the phonon modes at high symmetry points **M**(**qq0**) and **R**(**qqq**) at the Brillouin zone boundary. The present PDC in (**q00**) direction even does not show any inclination of the softening which is not a serious drawback looking to the simplification of the approach and success in predicting the mode instability at the **M** point of the BZ that has been predicted by both DFT calculations. The unstable modes at the **M** point of the BZ represent pure vibrations of the Ni atoms with all other atoms at rest.[21] Regarding the contradicting magnitude of the phonon modes due to the vibrations of the Mg atoms in two different DFT calculations, the present calculation supports the results of Heid *et al.*[21] Therefore, it appears that the contradicting magnitude of the phonon modes due to Mg atoms (35 meV) are overestimated in the LMTO calculations of Ignatov *et al.*[18] which predicts about 29% more at 45 meV. It can also be seen from the phonon dispersion curves that the vibrations of Ni atoms are not only responsible for the instability of the low-frequency acoustic modes but also for a few more lower optical phonon modes involving the Ni atom vibrations. A comparison between the present PDC and earlier calculated PDCs by using density functional theories[18,21] reveals that the gross features of the present PDC is closer to the DFT calculations of Heid *et al.*,[21] particularly in reproducing the unstable modes in two high symmetry directions of the BZ and hybridization between phonon modes due to Mg and Ni atoms. The phonon modes due to the carbon atoms in the present PDC are consistent with both previously investigated DFT phonon dispersion curves.

The phonon density of states is an important dynamical property, as its computation needs phonon frequencies in the entire Brillouin zone and can be defined as

$$g(\omega) = \frac{1}{N}\int_{BZ} \sum_j \delta[\omega - \omega_j(\vec{q})]d\vec{q}, \quad (3)$$

where N is a normalization constant that $\int g(\omega)d\omega = 1$. $g(\omega)d\omega$ is the ratio of the number of eigenstates in the frequency interval $(\omega, \omega + d\omega)$ to the total number of eigenstates. $\omega_j(\vec{q})$ is the phonon frequency of the jth phonon modes. The calculated total phonon density of states (DOS) of intermetallic $MgCNi_3$ superconductor has been presented in Fig. 3 along with the partial phonon density of states of constituent atoms of the $MgCNi_3$. The latter are used to calculate the vibrational amplitudes of the different atoms as presented in Table III, while the former are used to calculate the specific heat and Debye temperature. The partial phonon density of states contains information about the vibrational behavior of each atom and involves phonons in the entire Brillouin zone. To compare with the experimental data obtained from the inelastic neutron-scattering measurement, we have computed the neutron weighted phonon density of states (generalized phonon DOS). The generalized phonon density of states (GDOS) implies a weighting of vibrational modes by σ/m, where σ is scattering cross section and m is mass of the different species. The quantity for the atoms C, Mg, and Ni is 0.46, 0.179, and 0.31 barn/amu, respectively.[21] Figure 4 displays the present calculated GDOS [panel (b)] along with the experimentally obtained and DFT calculated GDOS (Ref. 21) [panel (a)] of $MgCNi_3$. It can be seen from Figs. 3 and 4, that the present study is quite successful in predicting the very important and remarkable feature, i.e., the presence of phonon DOS at 0 meV. It can be seen from the inset figure that the DOS is even present below 0 meV and there is a finite DOS at 0 meV. This is justified as there are low-frequency unstable modes having the negative frequencies over a large area in reciprocal space and is most prominent at zone boundary points. The similar results are obtained in experimental and DFT calculated DOS.[21] To understand the origin of the peaks in the DOS and the success of the present predictions, the results of partial DOS and total DOS displayed in Fig. 3 are examined. It can be seen from the critical assessment of these figures that there are three regions in the density of states: (1) below 25 meV, (2) 25 to 45 meV, and (3) 75 meV onwards. The first region below 25 meV is due to Ni and Mg atoms where the maximum contribution is due to Ni atoms as can be seen from the partial DOS. The situation is similar in second region but the contribution from C atoms is also appreciable. In the second region, a sharp peak near 35 meV is observed consistent with the DFT calculated GDOS and experimental inelastic neutron scattering data[21] which is mostly due to Mg participation and a small contribution from Ni vibrations. The final region in the higher-energy side of the spectra is due to the lighter atom carbon only. Figure 4 reveals that the present calculated GDOS is in good agreement with the experimental data[21] in the whole frequency range of spectra. It can also be noticed that the present simple calculation is more successful in reproducing the special features in low energy INS spectra of $MgCNi_3$ than the DFT calculations. The present computation is able to produce shoulders on both sides of the main peak near 20 meV in the low-energy region similar to the INS data. In conclusion, the present simple model has enabled an interpretation of the experimental INS data at the microscopic level.

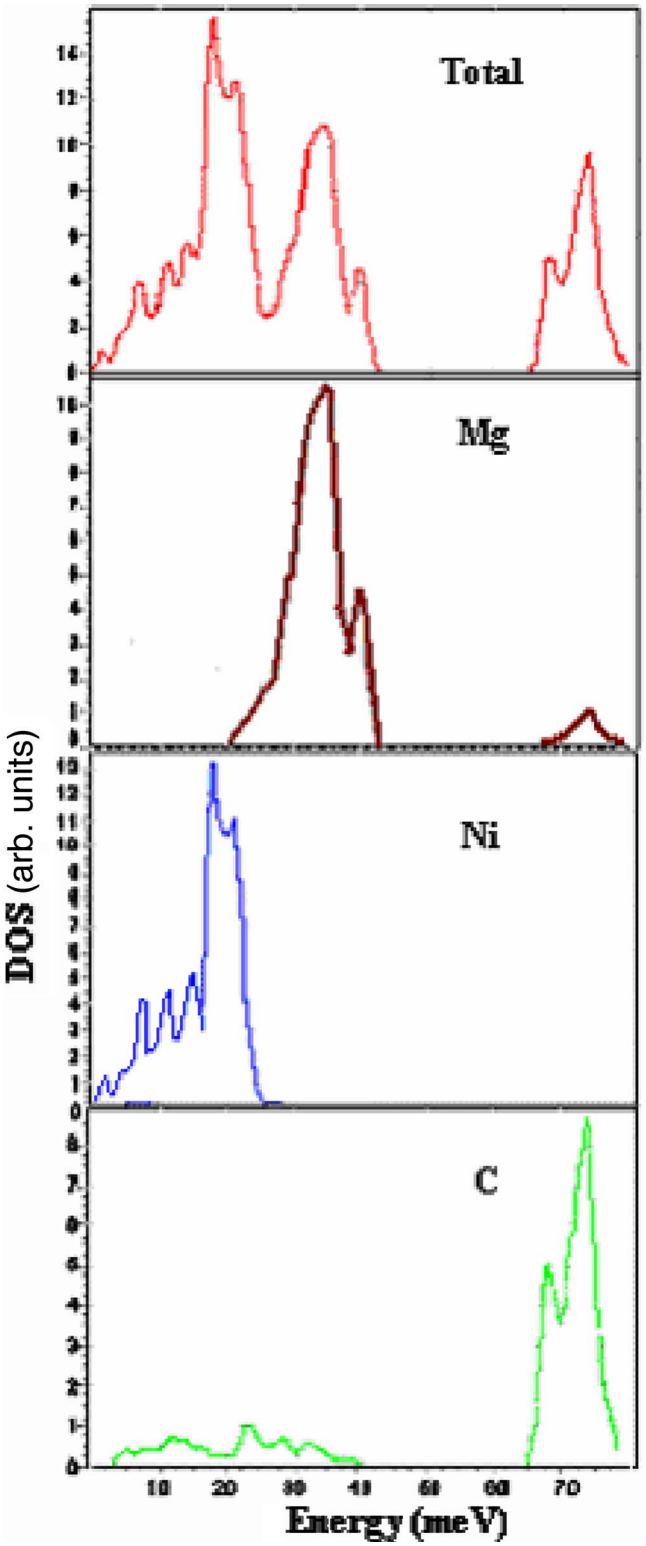

FIG. 3. (Color online) Computed total phonon density of states of $MgCNi_3$ and partial phonon density of states of the various atoms in $MgCNi_3$.

TABLE III. Vibrational amplitudes of the various atoms in $MgCNi_3$ with temperature.

	$8\pi^2\langle u^2\rangle/3$ (Å^2)					
Atoms	2 K	20 K	50 K	100 K	200 K	300 K
Mg	0.1541	0.1578	0.1778	0.2276	0.3526	0.4800
C	0.72	0.7227	0.7539	0.9345	1.5039	2.1531
Ni	0.1600	0.2100	0.3557	0.6041	1.1500	1.7000

A remarkable feature that is noticed from the phonon DOS similar to the dispersion curves of $MgCNi_3$ is the significant mixed character of phonons particularly in the low-frequency region. The significant mixed character of phonons is responsible for the renormalized phonons[25] arising due to the coupling between electrons and phonons. This suggests that the $MgCNi_3$ can be categorized as a strong electron-phonon coupling compound. A similar conclusion has been drawn from the previously reported DFT calculation[18,21–23] and specific-heat measurements.[3,8]

The calculated density of states is used to obtain the lattice specific heat at constant volume C_V in $MgCNi_3$, which is defined as

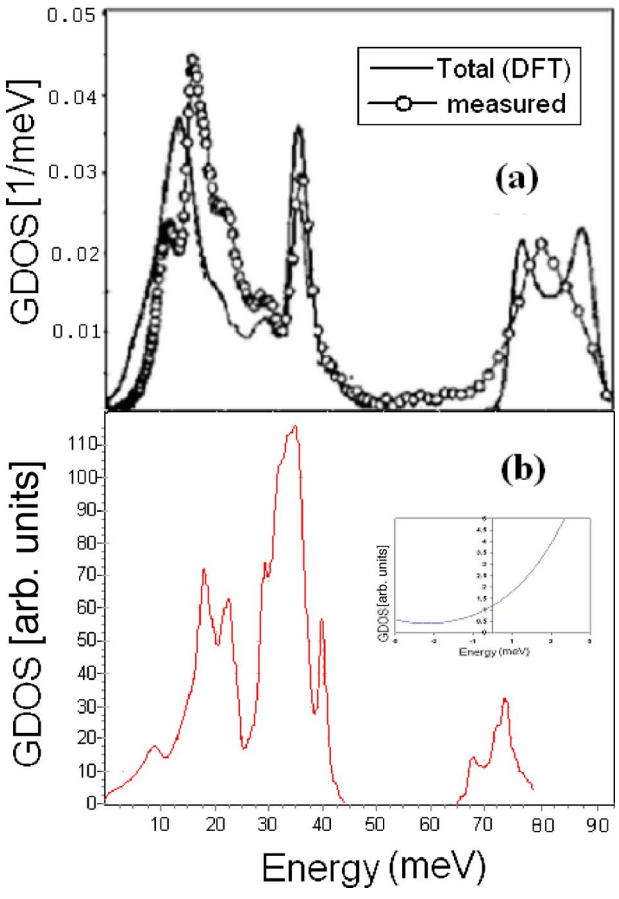

FIG. 4. (Color online) (a) The experimental inelastic neutron scattering data and computed generalized phonon density of states by using density functional theory. (b) Computed generalized phonon density of states of $MgCNi_3$ by using present model. The inset shows the presence of phonon DOS at 0 meV.

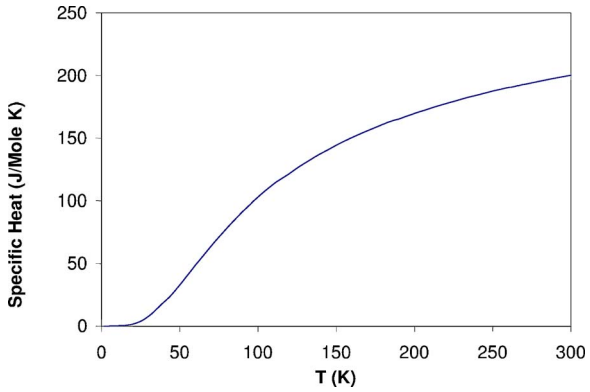

FIG. 5. (Color online) Lattice specific heat at constant volume of $MgCNi_3$ as a function of temperature.

$$C_V(T) = \frac{1}{N}\sum_{n,q}\left[\frac{h\omega_n(q)}{4k_BT\,sin\,h\left(\frac{h\omega_n(q)}{2k_BT}\right)}\right]^2. \quad (4)$$

This is a specific value of specific heat at constant volume. The temperature-dependent lattice specific heat at constant volume presented in Fig. 5 does not show any anomalous behavior in the temperature range of 2 to 300 K and is similar to the superconducting compounds belonging to the group of conventional superconductors. The computed specific heat which shows the classical behavior is in general good agreement with the experimental data[3,8] within the limitations of the present approach.

The computed partial phonon density of states is used to evaluate the vibrational amplitudes of the different species of $MgCNi_3$ compound and is presented in Table III. Table III reveals that the vibrational amplitudes increase with increase in temperature consistent with the Debye Waller factor derived from the neutron scattering[26] and EXAFS results.[17] The vibrational amplitudes do not behave anomalous in the studied temperature range.

IV. CONCLUSION

The present paper reports a systematic and detailed study on the zone center phonon frequencies, phonon dispersion curves, partial and total phonon density of states and thermodynamical properties for the $MgCNi_3$ intermetallic superconductor by using a simple lattice dynamical model under the framework of the rigid ion model. These results have been discussed in light of earlier performed DFT calculations and inelastic neutron scattering experiments.[19,21] An overall consistent description of the reported phonon properties for $MgCNi_3$, which compares well, in general, with the available theoretical and experimental data, is obtained. A remarkable soft mode behavior in the low-frequency region is observed similar to the DFT calculations by using a simple lattice dynamical model theory based on physically reliable model parameters. From the analysis of the phonon dispersion curves, partial and total phonon density states, it can be concluded that there is an appreciable hybridization of phonon

modes which reflects that the $MgCNi_3$ compound is a conventional BCS superconductor with a strong electron-phonon interaction. The thermodynamical properties show the BCS-like characteristics.

Finally, the main aim of this paper is to point out the behavior of phonons and allied properties in $MgCNi_3$ and clarify whether the superconductivity is governed by the BCS mechanism. The results show that the present simple lattice dynamical model calculation of $MgCNi_3$ realistically describes gross features of phonon spectra and provides some physics insight into their origins. From the present study, it is concluded that the superconductivity in $MgCNi_3$ is governed by the BCS mechanism.

ACKNOWLEDGMENTS

This work was supported by grants from the Department of Science and Technology (DST), Government of India and University Grant Commission. The author is extremely grateful to Dr. Mikhail Smirnov for making available his lattice dynamical code LADY. The author is also grateful to the TWAS and CBPF, Rio de Janeiro, Brazil for the hospitality and financial support.

[1] T. He, Q. Huang, A. P. Ramirez, Y. Wang, K. A. Regan, N. Rogodo, M. A. Heyward, M. K. Haas, J. S. Slusky, K. Inumaru, H. W. Zandbergen, N. P. Ong, and R. J. Cava, Nature (London) **411**, 54 (2001).

[2] H. Rosner, R. Weht, M. D. Johannes, W. E. Pickett, and E. Tosatti, Phys. Rev. Lett. **88**, 027001 (2002).

[3] J.-Y. Lin, P. L. Ho, H. L. Huang, P. H. Lin, Y.-L. Zhang, R.-C. Tu, C. Q. Jin, and H. D. Yang, Phys. Rev. B **67**, 052501 (2003).

[4] P. M. Singer, T. Imai, T. He, M. A. Hayward, and R. J. Cava, Phys. Rev. Lett. **87**, 257601 (2001).

[5] Z. Q. Mao, M. M. Rosario, K. D. Nelson, K. Wu, I.-G. Deac, P. Schiffer, Y. Liu, T. He, K. A. Regan, and R. J. Cava, Phys. Rev. B **67**, 094502 (2003).

[6] R. Prozorov, A. Snezhko, T. He, and R. J. Cava, cond-mat/0302431 (unpublished).

[7] K. Voelker and M. Sigrist, cond-mat/0208367 (unpublished).

[8] S.-H. Park, Y. W. Lee, J. Giim, Sung-Hoon Jung, H. C. Ri, and E. J. Choi, Physica C **400**, 160 (2000).

[9] R. Nagrajan *et al.*, Phys. Rev. Lett. **72**, 274 (1994).

[10] R. J. Cava *et al.*, Nature (London) **367**, 252 (1994).

[11] W. E. Pickett and D. J. Singh, Phys. Rev. Lett. **72**, 3702 (1994).

[12] L. F. Matthis, Phys. Rev. B **49**, 13279 (1994).

[13] G. Hislscher and H. Michor, in *Studies on High Temperature Superconductors*, edited by A. V. Narlikar (Nova Science Publishers, New York, 1999), Vol. 28, p. 246.

[14] P. Dervenaga, M. Bullock, J. Zarestky, P. Canfield, B. K. Cho, B. Haroon, A. I. Goldman, and C. Stassis, Phys. Rev. B **52**, R9839 (1995).

[15] F. Gompf, W. Reichardt, H. Schober, B. Renker, and M. Buchgeister, Phys. Rev. B **55**, 9058 (1997).

[16] J. Zarestky, G. Stassis, A. Coldman, P. Canfield, G. Shirane, and S. Shapiro, Phys. Rev. B **60**, 11932 (1999).

[17] A. Yu. Ignatov, L. M. Diong, T. A. Tyson, T. He, and R. J. Cava, Phys. Rev. B **67**, 064509 (2003).

[18] A. Ignatov, S. Y. Savrasov, and T. A. Tyson, cond-mat/0304466 (unpublished).

[19] A. Yu Ignatov, Nucl. Instrum. Methods Phys. Res. A **448**, 322 (2000).

[20] J. B. Boyce, F. G. Bridges, T. C. Clarson, T. H. Geballe, G. G. Li, and A. N. Slright, Phys. Rev. B **44**, 6961 (1991).

[21] R. Heid, B. Renker, H. Schober, P. Adelmann, D. Ernst, and K.-P. Bohnen, cond-mat/0310592 (unpublished).

[22] J. H. Shim, S. K. Kwon, and B. I. Min, Phys. Rev. B **64**, 180510 (2001).

[23] D. J. Singh and I. I. Mazin, Phys. Rev. B **64**, 140507 (2001).

[24] M. B. Smirnov and V. Yu. Kazimirov (unpublished).

[25] W. Weber, Phys. Rev. Lett. **58**, 1371 (1987).

[26] Q. Huang, T. He, K. A. Regan, N. Rogado, M. A. Hayward, M. K. Haas, K. Inumaru, and R. J. Cava, cond-mat/0105418 (unpublished).